Food Bioscience 78 (2026) 108444

Contents lists available at ScienceDirect

Food Bioscience

journal homepage: www.elsevier.com/locate/fbio

Uncovering bacterial–fungal relationships in *Meju* fermentation through relative and absolute abundance-based metagenomic analysis

Eunhye Jo [a], Sungmin Hwang [b], Hyeyoung Lee [c], Jaeho Cha [a,d,*]

[a] Department of Microbiology, Pusan National University, Busan, 46241, Republic of Korea
[b] Division of Convergence on Marine Science, Korea Maritime & Ocean University, Busan, 49112, Republic of Korea
[c] Department of Food Science and Technology, Dong-eui University, Busan, 47340, Republic of Korea
[d] Microbiological Resources Research Institute, Pusan National University, Busan, 46241, Republic of Korea

ARTICLE INFO

Keywords:
Bacterial–fungal interaction
Microbial community
Amplicon-based sequencing
Absolute abundance
Traditional soybean fermented food

ABSTRACT

Traditional Korean *Meju*, a key ingredient for fermented soybean foods such as *Doenjang* and *Ganjang*, undergoes complex microbial fermentation driven by diverse bacteria and fungi. Although microorganisms are known to play essential roles in the flavor, safety, and nutritional quality of *Meju*, most studies relying on relative abundance data provide limited insight into their true interactions. This study investigated bacterial-fungal interactions during three stages of *Meju* fermentation using absolute abundance data derived from quantitative PCR (qPCR) integrated with amplicon-based sequencing. Physicochemical changes, including pH, water content, and amino nitrogen, were monitored to track fermentation progress. Amplicon-based sequencing revealed distinct patterns of relative abundance in bacterial and fungal communities, as assessed by Shannon and Chao1 indices. *Bacillus* dominated the bacterial community throughout the entire fermentation period, whereas *Rhizopus* and *Mucor* were predominant in the fungal community. Quantitative PCR analysis revealed a significant increase in microbial biomass, from 1.01×10^8 to 2.15×10^{11} copies/g for bacteria and from 9.49×10^6 to 2.53×10^{10} copies/g for fungi. Integration of qPCR-based quantitative data with relative abundance revealed a significant positive correlation between *Bacillus* and *Rhizopus* that was undetectable using relative data alone. These findings demonstrate that integrating absolute abundance with sequencing data provides novel insights into microbial dynamics and interkingdom interactions during *Meju* fermentation, contributing to a deeper understanding of fermentation ecology in soybean-based foods.

1. Introduction

Meju, a traditional Korean fermented soybean brick, serves as a key ingredient in soybean pastes (*Doenjang*) and soy sauce (*Ganjang*). It is produced by steaming, mashing, and molding soybeans, following by fermentation. Traditional *Meju* fermentation occurs in environments rich in diverse microorganisms, whereas modernized *Meju* undergoes controlled inoculation for consistent quality (Kim et al., 2013, 2017). In traditional *Meju*, fermentation conditions such as temperature and duration vary across households and manufacturers, typically involving two or three stages depending on environmental factors such as temperature and humidity (Shin & Jeong, 2015). In the traditional production of *Meju*, soybeans are first boiled, mashed, and molded into brick-shaped forms. These blocks undergo a multi-step fermentation process. The first step is a drying stage conducted in a fermentation room. Subsequently, the blocks are bound with rice straw and fermented outdoors, representing the second stage. Finally, the *Meju* is transferred indoors and fermented under warm conditions, completing the third stage of the process. Fermentation is carried out either in indoor fermentation rooms or under open-air conditions, reflecting different traditional practices. This process fosters a complex microbial ecosystem composed primarily of bacteria and fungi, which collectively shape the flavor, safety, and nutritional quality of soybean-based fermented foods.

Advances in sequencing technology have facilitated both culture-dependent and culture-independent studies, enabling the characterization of key microbes involved in soybean fermentation. For example, metagenomic analyses of *Meju* have revealed diverse bacterial genera such as *Bacillus*, *Enterococcus*, *Weissella*, *Lactococcus*, *Leuconostoc*, and *Staphylococcus* (Jo et al., 2024; Kim et al., 2022; Lee et al., 2024). Among these, *Bacillus* species are particularly well known for their protease and

* Corresponding author. 2 Busandaehak-ro 63beon-gil, Geumjeong-gu, Busan, 46241, Republic of Korea.
E-mail address: jhcha@pusan.ac.kr (J. Cha).

https://doi.org/10.1016/j.fbio.2026.108444
Received 14 November 2025; Received in revised form 31 January 2026; Accepted 7 February 2026
Available online 10 February 2026

lipase activities, which degrade soybean proteins and fats into peptides, amino acids, and free fatty acids, thereby enhancing the flavor and nutritional value of fermented soybean products (Na et al., 2022). Likewise, fungal genera including *Aspergillus, Mucor, Rhizopus,* and *Penicillium* significantly contribute to soybean fermentation by producing enzymes such as amylases and proteases, which breakdown complex carbohydrates and proteins, leading to desirable textures, flavors, and bioactive compounds (Elhalis et al., 2024; Kim et al., 2024; Sun et al., 2019). During fermentation, microorganisms play essential roles through their mutual interactions (Singh et al., 2022; Song et al., 2020, 2021).

Despite their significance, the current understanding of bacterial-fungal interactions in *Meju* is limited. Most studies on microbial communities during *Meju* fermentation depend on relative abundance data, which have limitations in accurately interpreting microbial dynamics. (Bruijning et al., 2023). Correlation analysis based solely on relative abundance data is susceptible to spurious results due to the compositional nature of the data, where an increase in one taxon may appear as a decrease in another. Moreover, such approaches fail to capture changes in total microbial biomass (Shanahan & Hill, 2019). Even when the relative proportion of microorganisms remains constant, their ecological impact may vary depending on the overall biomass, highlighting the importance of incorporating absolute abundance data in microbial community studies. In microbial ecology, combining relative and absolute abundance provides a more comprehensive approach, facilitating more accurate evaluations of microbial taxonomic and functional dynamics (Props et al., 2017; Yang et al., 2025). Absolute quantification can be achieved through quantitative polymerase chain reaction (qPCR), digital PCR (ddPCR), flow cytometry, or next-generation sequencing (NGS)-based approaches with internal/external spike-in controls (Harrison et al., 2021; Kallastu et al., 2023; Vandeputte et al., 2017). These complementary techniques allow for the measurement of actual microbial abundance, providing more reliable ecological interpretations and facilitating the identification of factors driving community shifts. In soybean-based fermented foods, it is important to accurately assess microbial ecology by considering the increasing microbial biomass during fermentation. The limitations of relative abundance analysis can be complemented by incorporating absolute abundance measurements.

Therefore, this study aimed to investigate bacterial–fungal relationships during traditional *Meju* fermentation by integrating amplicon-based sequencing with qPCR provides the sensitivity, specificity, and accessibility for absolute microbiome quantification, particularly in assessing dynamic changes in bacterial populations. By employing both relative and absolute quantification methods to comprehensively evaluate microbial correlations, we sought to uncover microbial associations—particularly between dominant taxa—and to provide a more quantitative understanding of microbial interaction in traditional Korean fermented soybean.

2. Materials and methods

2.1. Sample preparation

All *Meju* samples used in this study were produced at a facility in Gyeongju, South Korea, using traditional methods without intentional microorganism inoculation (Jina F&C). The soybeans (*Glycine max* (L.) Merr.), specifically the Daewon cultivars, were harvested in Mungyeong, South Korea. A total of 60 kg of soybeans were washed, soaked overnight, boiled for 6 h, and then cooled for 4 h (Fig. S1). The prepared soybeans were mashed and shaped into brick-like blocks measuring 20 cm × 13.5 cm × 10.5 cm, each weighing 2.5 kg. A total of 45 *Meju* samples were included in this study, with sampling conducted at 15 time points. At each sampling point, three biological replicates were collected. First, the drying stage has conducted for 5 days in which temperature and humidity were controlled at 18–23 °C and 50 ± 5%, respectively. The first fermentation stage, conducted under open-air conditions, lasted for 28 days following the drying process. During the second fermentation stage, the *Meju* was incubated under controlled conditions in a fermentation room with a temperature range of 37–40 °C and humidity maintained at 65 ± 5% for 15 days. A total of 15 sampling events were conducted, with three *Meju* samples collected each time. After homogenizing, the samples were stored in petri dishes, and ten plates were preserved at −80 °C for further analysis.

2.2. Physicochemical determination

To evaluate the physicochemical properties of *Meju*, measurements of water content, pH, and amino-type nitrogen content were conducted according to the previously reported methods (Heo et al., 2023; Ryu et al., 2021; Yang et al., 2023).

2.2.1. Water content measurement

The water content of *Meju* was determined using a freeze-drying method. First, the weight of an empty petri dish was recorded. Then, a portion of homogenized *Meju* was placed into the dish and weighed. The sample was frozen at −80 °C, followed by moisture removal using a freeze dryer. After the sample weight stabilized, the final weight was recorded, and the water content was calculated based on the difference between the initial and final weights. Each *Meju* sample was analyzed in triplicate using three petri dishes.

2.2.2. pH measurement

To measure pH, 5 g of homogenized *Meju* were diluted with 20 mL of deionized water. The mixture was vortexed at 1,500 g for 10 min, after which additional deionized water was added to adjust the total volume to 50 mL. The mixture was then centrifuged at 3,500 g for 20 min, and the resulting supernatant was collected. The pH was measured using a pH meter (Mettler Toledo, OH, USA).

2.2.3. Amino-type nitrogen content measurement

Amino-type nitrogen content was determined using the formol titration method (Ryu et al., 2021; Taylor, 1957). One gram of *Meju* was mixed with 50 mL of deionized water and stirred for 30 min. The sample was then titrated with 0.1 N NaOH until the pH reached 8.4, and the required volume of NaOH was recorded. Following this, 20 mL of formalin solution (37% (v/v) formaldehyde, pH 8.3) was added, and the titration continued with 0.1 N NaOH until the pH once again reached 8.4. A preliminary test was conducted using distilled water, and the volume of 0.1 N NaOH consumed was recorded for calculation.

2.3. Construction of MiSeq library

Total genomic DNA was extracted using the NucleoSpin Mini kit for DNA from soil (Macherey-Nagel, Düren, Germany) following the manufacturer's instructions. To perform amplicon sequencing, the V5-V6-V7 regions of the 16S rDNA were amplified using the primers 799F (5′–AACMGGATTAGATACCCKG–3′) and 1193R (5′–ACGTCATCCCC ACCTTCC–3′), which were specifically selected to minimize the amplification of chloroplast DNA and mitochondrial DNA (Beckers et al., 2016). For the analysis of the fungal community, the ITS86F (5′–GTGAATCATCGAATCTTTGAA–3′) and ITS4 (5′–TCCTCCGCTTA TTGATATGC–3′) primers were used to target the ITS2 region (Op De Beeck et al., 2014). The primers were designed with Illumina sequencing adapters, including forward (5′–TCGTCGGCAGCGTCAGAT GTGTATAAGAGACAG–3′) and reverse (5′–GTCTCGTGGGCTCGGAGA TGTGTATAAGAGACAG–3′) sequences. A total of 10 μg of genomic DNA was used for amplification, and the resulting amplicons were then purified using the Expin™ PCR SV kit (GeneAll Biotechnology, Korea) to remove impurities and ensure high-quality DNA. To prepare for sequencing, indexing PCR was performed using 5 μL of the purified amplicon, which was further extended with Illumina-specific adapters. All PCR reactions were carried out in a 20 μL reaction volume,

containing 10 μL of 2 × Prime Taq Premix (Genetbio, Korea), 1 μL of each primer (10 μM), 1 μL of template DNA (5 ng/μL), and distilled water to make up the final reaction volume. The first round of PCR was conducted under the following thermal cycling conditions: an initial denaturation at 95 °C for 3 min, followed by 35 cycles of denaturation (95 °C for 30 s), annealing (55 °C for 30 s), and extension (72 °C for 30 s), with a final extension at 72 °C for 5 min. After amplification, the PCR products were purified using the Expin™ PCR SV Kit to eliminate contaminants. A second PCR was then performed for indexing, following the same conditions as the first PCR, except that the number of cycles was reduced to eight. The indexed amplicons were verified using 1% agarose gel electrophoresis to confirm the expected product size and purity. The final quantification of the amplicons was carried out using a Nanodrop spectrophotometer. Once purified and indexed, the amplicon libraries were pooled in equal amounts and subjected to sequencing using the Illumina MiSeq platform, generating paired-end reads (2 × 300 bp). Sequencing was performed at Macrogen (Korea).

2.4. Bioinformatic processing and microbial diversity analysis

The raw sequence data underwent quality control using FastQC, and sequences were trimmed to retain only regions with a quality score above Q30 (Andrews, 2017). The trimming parameters were set to truncLen = c(270, 210) for 16S rRNA and truncLen = c(200, 165) for ITS. To generate amplicon sequence variants (ASVs), raw reads were denoised, merged, and filtered to remove chimeric sequences using the DADA2 package (version 1.24.0) (Callahan et al., 2016). Taxonomic classification of each ASV was conducted using the Phyloseq package (version 1.36.0) (McMurdie & Holmes, 2013), with the SILVA database (version 132) employed for bacterial 16S rRNA gene sequences and the UNITE database (release 10.05.21) used for fungal ITS regions (Nilsson et al., 2019; Quast et al., 2012). ASVs annotated as 'Mitochondria' (family level) and 'Chloroplast' (order level) were removed from the bacterial dataset. For the fungal dataset, non-fungal taxa ('k_Viridiplantae' and 'k_Eukaryota_kgd_Incertae_sedis') were excluded. α-Diversity indices, including Chao1 richness and Shannon diversity, were calculated based on ASV data for each sample. To assess differences in microbial community composition, principal coordinate analysis (PCoA) was conducted based on a Bray–Curtis dissimilarity distance matrix. All bioinformatics analyses were performed in the R environment (version 4.2.1).

2.5. Quantification of microorganisms

To assess viable microorganisms in *Meju*, both culture-dependent and culture-independent methods were employed, including plate cell count and qPCR. The culture-dependent assay was conducted according to a previously described procedure (Han et al., 2024). 0.5 g of each *Meju* sample was diluted in 5 mL of 1 × Phosphate-Buffered Saline (PBS) to achieve a final concentration of 0.1 g/mL. The samples were vortexed for 10 min to ensure particle suspension. Serial 10-fold dilutions were prepared in 1 × PBS, and 100 μL of each dilution was spread onto the appropriate agar plates. Tryptic Soy Agar (TSA), De Man–Rogosa–-Sharpe agar (MRS), Potato Dextrose Agar (PDA), and Yeast extract Peptone Dextrose (YPD) plates, each containing 1.5% (w/v) agar, were used to cultivate bacteria, lactic acid bacteria, yeasts, and fungi, respectively. PDA and YPD plates were supplemented with 60 μg/mL chloramphenicol to inhibit bacterial growth. All culture-dependent assays were conducted under aerobic conditions, with TSA and MRS plates incubated at 37 °C and PDA and YPD plates incubated at 30 °C. Colony-forming units (CFUs) per gram of *Meju* were calculated by counting colonies in the range of 30 to 300 on the plates and multiplying by the dilution factor.

For the culture-independent assay, qPCR was conducted to determine the DNA quantity according to the previously reported method (Jung et al., 2014). The same primers described in Method 2.3, targeting the 16S rRNA gene for bacteria and the ITS gene for fungi, were used for this analysis. DNA quantification was performed using an Applied Biosystems StepOne real-time PCR system (Thermo Fisher Scientific, MA, USA). qPCR was conducted in 20-μL reaction volumes, consisting of 10 μL of TB Green Premix Ex Taq, 1 μL of each forward and reverse primer (2 μM), ROX 0.4 μL, DEPC water 6.6 μL, and 1 μL of template DNA. The qPCR conditions included an initial denaturation step at 95 °C for 1 min, followed by 30 cycles of denaturation at 95 °C for 30 s, annealing at 55 °C (for bacteria) or 50 °C (for fungi) for 30 s, and extension at 72 °C for 30 s (for bacteria) or 20 s (for fungi), followed by a final melting curve analysis. Absolute quantification was performed by comparing the quantification cycle (Cq) values of the samples against a standard curve generated from known copy numbers. The absolute abundance of each ASV was subsequently estimated by combining quantitative PCR data with ASVs profiles obtained from bioinformatic analysis, calculated as the product of total bacterial 16S rRNA gene copy numbers and relative abundance from high-throughput sequencing (Bubeck et al., 2020).

2.6. Statistical analysis

α-diversity indices, including Chao1 and Shannon indices, were used to evaluate differences among fermentation stages, and statistical significance was assessed using the Wilcoxon rank-sum test. A permutational multivariate analysis of variance (PERMANOVA) was conducted for β-diversity analysis using the adonis2 function in the Vegan package (version 2.6-6.1) with fermentation stage specified as the explanatory variable, using 999 permutations and a fixed random seed to ensure reproducibility. Spearman correlation analysis was conducted to assess the relationships between dominant bacterial and fungal taxa using the Hmisc package (version 4.7.1) in R (Harrell & Dupont, 2019). Correlations were considered significant when the Spearman correlation coefficients ($|\rho| > 0.8$) and p-value ($p < 0.05$) criteria were met. The resulting positive and negative correlations among microorganisms were visualized using the corrplot package (version 0.92) in R.

2.7. Sequencing data accession number

The bacterial and fungal metagenome sequence data generated in this study have been deposited in the NCBI Short Read Archive (SRA) under BioProject accession numbers PRJNA1218301.

3. Results

3.1. Dynamics of physicochemical properties and microbial communities during successive stages of Meju fermentation

To effectively monitor microbial dynamics throughout fermentation, samples were collected more frequently at the beginning of each stage, when rapid microbial proliferation was expected (Fig. 1A). The drying stage, which lasted for five days, aimed to reduce surface moisture from the shaped soybean blocks. Following the drying process, the first fermentation stage lasted for 28 days, during which the growth of autochthonous microorganisms was facilitated by exposure of the *Meju* blocks to the natural environment. According to Weather Forecast records, the ambient humidity during this period was 50.9 ± 15.46%, with temperatures ranging from −5 to 12 °C during the 28 days. The second fermentation stage was conducted under controlled conditions for 15 days. The surface appearance of *Meju* is changed during fermentation (Fig. 1B).

To monitor changes across the three fermentation stages, pH, water content, and amino-type nitrogen were analyzed (Fig. 2). Despite practical fluctuations in temperature and humidity across the three stages of the 48-day fermentation period, pH remained relatively stable, likely attributable to the buffering capacity of soybean substrates (Mennah-Govela et al., 2020). In contrast, water content steadily decreased, particularly during the drying and second fermentation

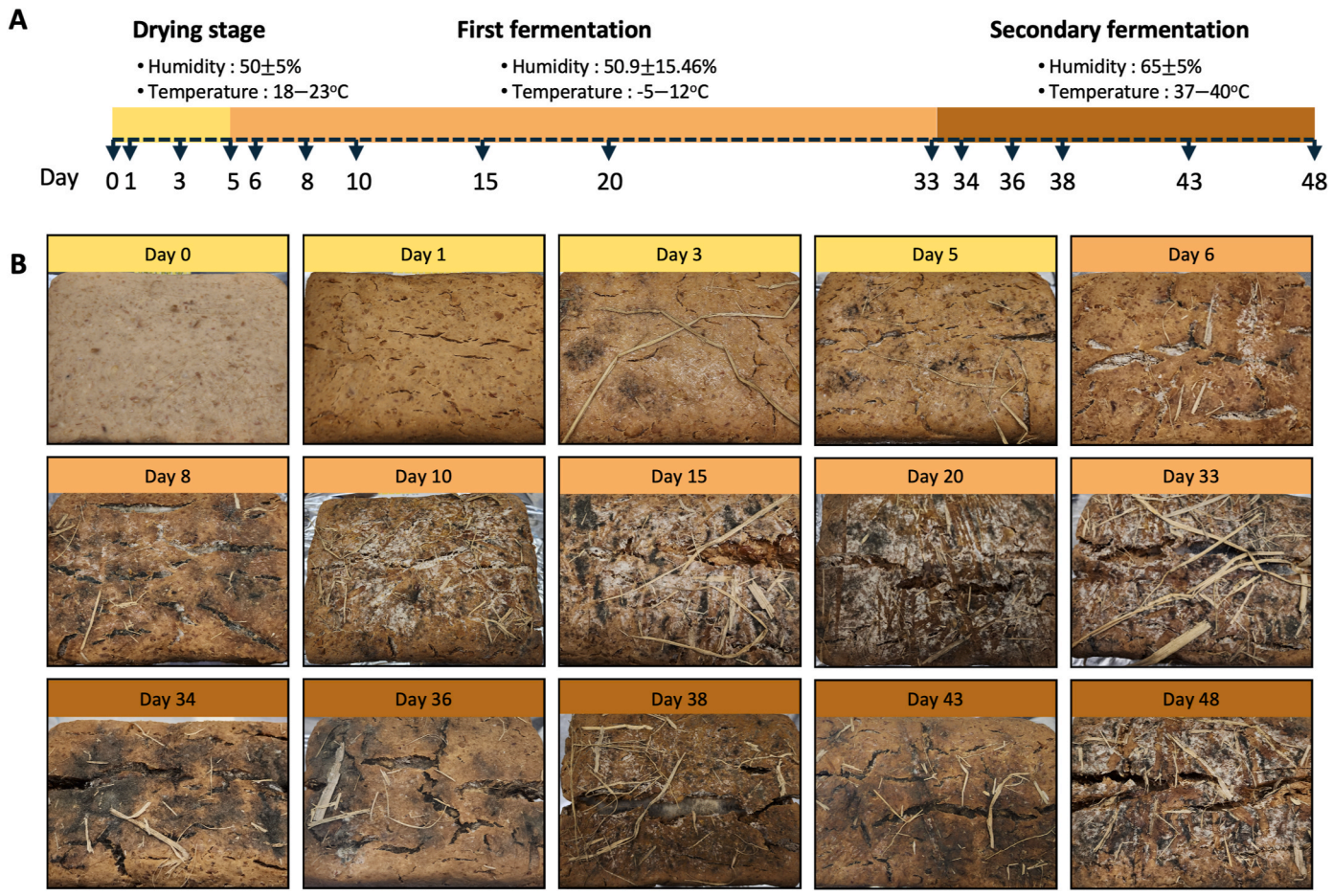

Fig. 1. Three fermentation stages and morphological variation of *Meju*. (A) Sampling time points (15 intervals) and fermentation conditions (humidity and temperature) are shown across the three fermentation stages: drying, first, and second. (B) Surface appearance of *Meju* during each stage is displayed, with colors transitioning from yellow to light brown and dark brown in the panel.

stages, where humidity was tightly controlled (Fig. 2A). Initial water content was approximately 60%, declining to an average of approximately 25% by the end of fermentation. Amino-type nitrogen, monitored by the Formol titration method, showed a continuous increase (Fig. 2B). The most pronounced rises occurred during the drying stage and the second fermentation stage, reflecting proteolytic activity and microbial metabolism that contribute to the flavor and nutritional development in *Meju*. Viable cells of bacteria, lactic acid bacteria, fungi, and yeast were enumerated using TSA, MRS, PDA, and YPD agar plates (Fig. 2C). TSA yielded the highest colony counts, approximately 10^9 CFU/g, indicating a substantial overall bacterial growth. In contrast, MRS plates revealed comparatively lower counts, suggesting lactic acid bacteria formed a smaller portion of the community despite high total biomass. In contrast, enumeration of cultivable fungi under bacteria-suppressed conditions revealed a steady increase throughout fermentation, converging at comparable levels of $\sim 10^4$ CFU/g on both YPD and PDA media.

DNA-based analyses using qPCR confirmed that bacterial populations consistently outnumbered fungi and yeast throughout the fermentation process (Fig. 2D). Bacteria showed a rapid increase during the initial drying stage, followed by stabilization during the first and second fermentation stages. Average values (±SD) increased from $1.51 \times 10^{10} \pm 1.79 \times 10^{10}$ copies/g during the drying stage to $9.52 \times 10^{10} \pm 4.97 \times 10^{10}$ copies/g and $9.54 \times 10^{10} \pm 6.02 \times 10^{10}$ copies/g in the first and second fermentation stages, respectively. In contrast, fungal biomass showed a higher average value during the first fermentation stage than during the second fermentation stage, with average (±SD) values of $4.59 \times 10^8 \pm 1.20 \times 10^9$ copies/g for the drying stage, $3.50 \times 10^9 \pm 6.42 \times 10^9$ copies/g for the first fermentation stage, and $2.68 \times 10^9 \pm 2.18 \times 10^9$ copies/g for the second fermentation stage. The elevated fungal biomass observed during the first fermentation stage was primarily attributed to a sharp increase at day 28, reaching $1.63 \times 10^{10} \pm 6.98 \times 10^9$ copies/g. This surge was likely driven by elevated humidity following rainfall. According to data from the Korea Meteorological Administration, precipitation of 3 mm and a relative humidity of 75.5% were recorded on the corresponding date. Additionally, fungal biomass increased in a manner consistent with the culture-based results (Fig. 2C), demonstrating complementary trends in fungal growth across the two experimental approaches.

3.2. Contrasting temporal patterns of bacterial and fungal diversity during Meju fermentation

To assess the abundance and diversity of bacterial and fungal communities during *Meju* fermentation, Chao1 and Shannon indices were analyzed based on ASVs (Fig. 3A and B, and Table S1). The Chao1 index of the bacterial community, which represents species richness, showed a pronounced increase during the drying stage (from 14 to 74) and continued to increase to a mean value of 96 in the first fermentation stage. A statistically significant difference was observed between the drying and first fermentation stages (Wilcoxon $p < 0.001$), whereas no significant change was detected during the second fermentation stage. The Shannon index, reflecting both richness and evenness, showed a continuous increase from the drying stage (mean 0.938) to the first fermentation stage (2.067) and further to the second fermentation stage (2.428), demonstrating a significant enhancement of bacterial diversity

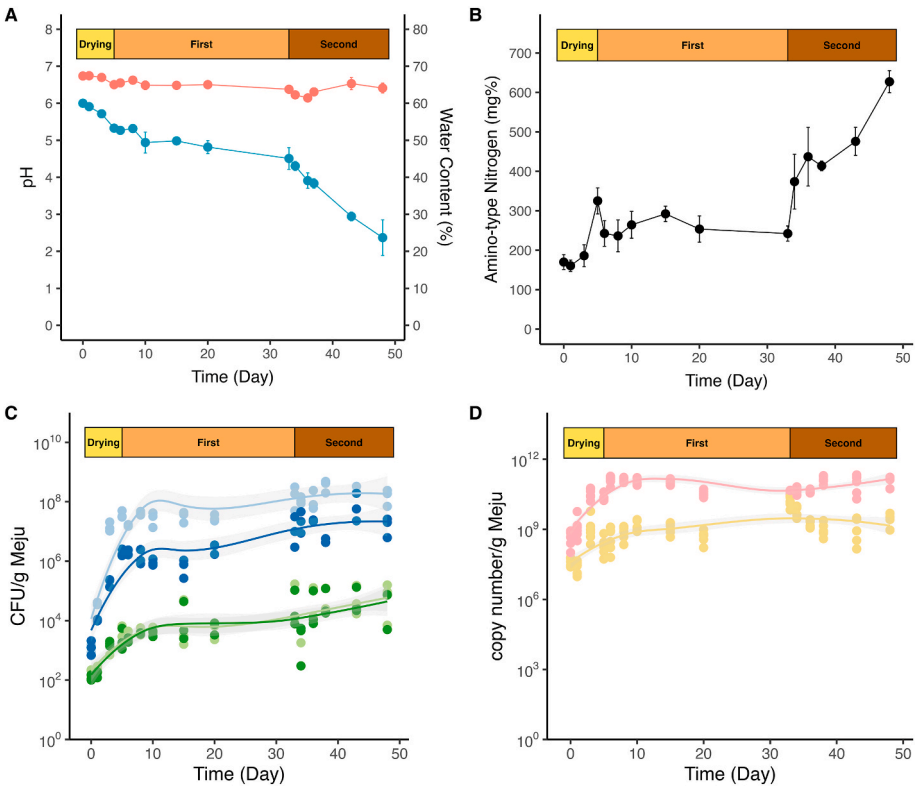

Fig. 2. Profiles of physicochemical properties and microbial populations. (A) Changes in pH (pink line, left y-axis) and water content (light blue line, right y-axis) across fermentation stages. Data represent the mean ± standard deviation (SD) of biological replicates. (B) Changes in amino-type nitrogen content, shown as mean ± SD of biological replicates. (C) Viable cell counts determined by plate culture on four media: TSA (light blue), MRS (blue), PDA supplemented with 60 μg/mL chloramphenicol (light green), and YPD supplemented with 60 μg/mL chloramphenicol (green). (D) Copy numbers of bacterial 16S rRNA genes (light pink) and fungal ITS regions (light yellow), normalized by dilution rate and sample weight.

across the fermentation stages. In contrast, the fungal community displayed a different pattern. The Chao1 index increased from 10 to 40 during the drying stage but showed no significant change thereafter, with average values of 29 and 26 during the first and second fermentation stages, respectively. However, the Shannon index exhibited a pronounced decrease from 2.393 in the drying stage to 1.633 and 1.180 in the first and second fermentation stages, respectively (Wilcoxon $p <$ 0.01). This reduction implies that despite relatively high fungal species richness, the advancing fermentation process led to reduced evenness and increased dominance by a small number of fungal taxa.

To further investigate $\beta-$diversity and temporal variations in microbial community structures, a Principal Coordinates Analysis (PCoA) was conducted (Fig. 3C and D). The bacterial community remained relatively stable during the drying stage but showed pronounced divergence beginning with the first fermentation stage. PERMANOVA confirmed significant stage-dependent differences in bacterial community composition ($R^2 = 0.40745$, $p = 0.001$), with PC1 and PC2 explaining 22.2% and 48.3% of the total variance, respectively. Similarly, significant stage-related differences were observed in the fungal community ($R^2 = 0.11983$, $p = 0.001$), with PC1 and PC2 accounting for 49.4% of the variation.

3.3. *Bacillus dominates the bacterial community, while fungal community composition varies during fermentation*

Taxonomic annotation of bacterial ASVs using the SILVA database identified a total of 819 ASVs (Table S2). ASVs that could not be assigned to a specific taxonomic group were designated as 'unidentified'. At the genus level, a total of 98 bacterial genera were identified, of which 19 genera, including 'unidentified', exhibited a relative abundance greater than 1% (Fig. 4A). *Bacillus* was the most prevalent genus throughout the fermentation process, although its relative abundance declined from 99.56 ± 0.28% on day 0 to 61.89 ± 13.45% on day 33. Despite this decline, *Bacillus* remained the dominant genus at all stages: 98.11 ± 2.17% in the drying stage, 82.13 ± 13.27% in the first fermentation, and 79.57 ± 11.34% in the second fermentation, respectively. Meanwhile, the relative abundances of *Lelliottia*, *Pantoea*, *Enterobacter*, and *Rahnella* increased during the first fermentation stage. Their abundance subsequently declined during the second fermentation stage, when controlled temperatures (37–40 °C) may have restricted their proliferation.

Taxonomic annotation of fungal ASVs identified 437 unique ASVs (Table S2). At the genus level, 113 taxa were identified, among which 35 genera exhibited a relative abundance greater than 2% (Fig. 4B). *Rhizopus* exhibited the highest relative abundance, increasing from 31.24 ± 10.07% on day 0 to 62.40± 25.90% on day 5 of the drying stage, and remained dominant (62.30± 6.83%) on day 20. *Mucor* and *Cladosporium* were also highly abundant, with *Mucor* showing a notable increase on day 33 (78.59 ± 14.76%), which may have been associated with elevated humidity levels caused by rainfall. However, its abundance declined during the second fermentation stage, while *Rhizopus* became more dominant again. Under controlled fermentation conditions in the second stage (65 ± 5% humidity, 37–40 °C), the relative abundances of *Rhizopus* and *Aspergillus* increased. In conclusion, metagenomic analysis based on relative abundance revealed that *Bacillus* remained the dominant genus in the bacterial community across all stages, whereas *Rhizopus* and *Mucor*, classified as Zygomycetes at the fungal phylum level, were predominant but showed fluctuating abundances depending on the fermentation stage.

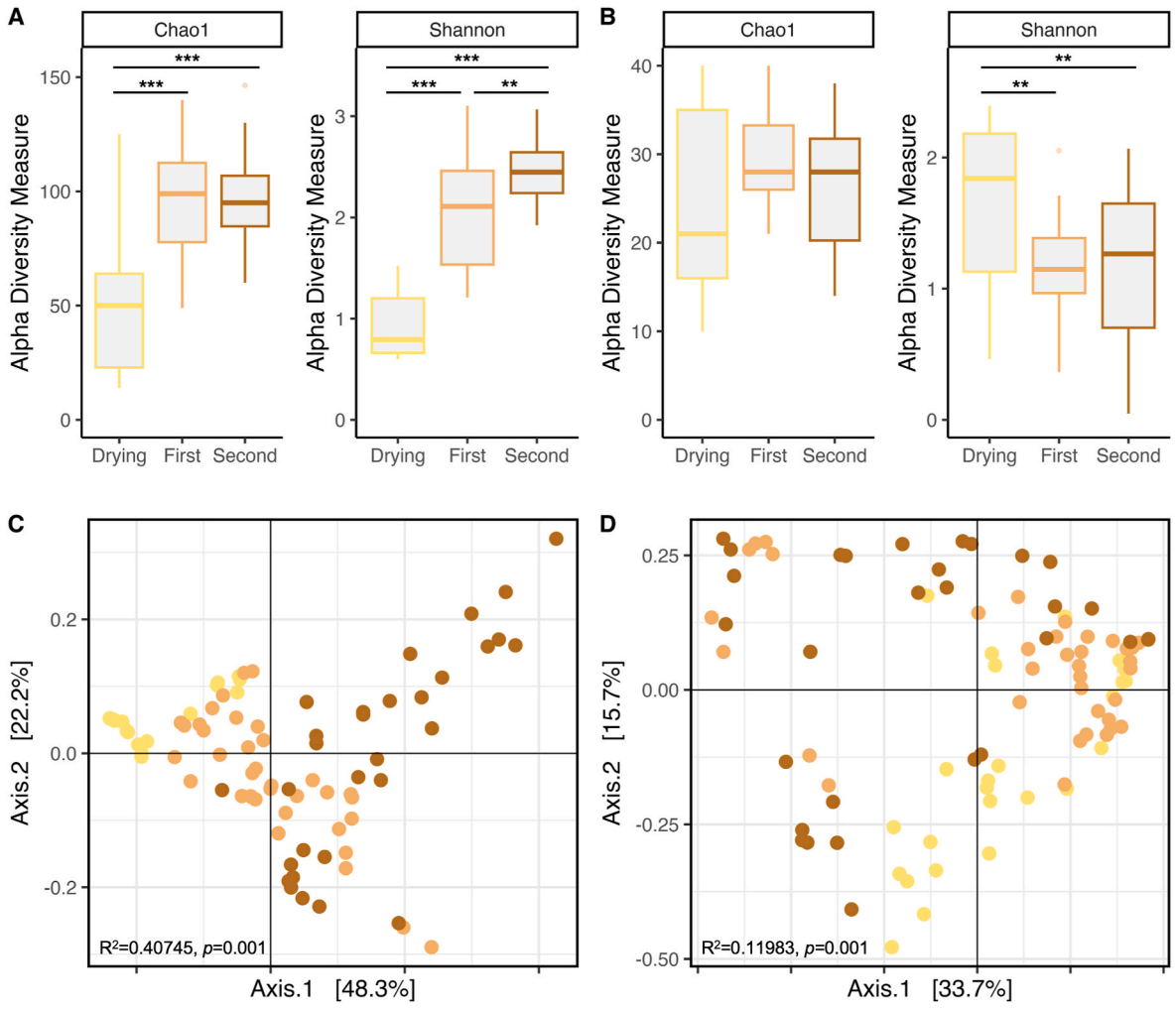

Fig. 3. ***α*-and *β*-diversity of bacterial and fungal communities.** *α*-diversity indices (Chao1 and Shannon) of bacterial (A) and fungal (B) communities. The yellow, orange, and brown boxplots represent the drying, first, and second fermentation stages, respectively. Statistical differences in *α*-diversity indices among fermentation stages were evaluated using the Wilcoxon rank-sum test, with significance levels indicated as $p < 0.05$ (*), $p < 0.01$ (**), and $p < 0.001$ (***). Principal Coordinate Analysis (PCoA) of bacterial (C) and fungal (D) communities, with fermentation stages color-coded. The axes represent dissimilarity values.

3.4. Integrating absolute and relative abundance data reveals stage-specific microbial dynamics

Relative abundance analysis, in which each sample was normalized to 100%, indicated shifts in community composition; however, this approach may be confounded by differences in microbial biomass across samples. Previous qPCR experiments in Result 3.1 demonstrated a significant increase in bacterial and fungal populations during the initial drying stage of fermentation (Fig. 2D). To address this, absolute abundance was estimated by multiplying relative abundance values by the corresponding quantitative data. At the genus level, including 'unidentified' taxa, the top ten genera were identified based on total abundance. Heatmap visualization revealed dynamic changes in absolute abundance across fermentation days (Fig. 5).

Comparison of absolute with relative abundance highlighted notable differences. For bacteria, relative abundance analysis indicated *Bacillus* dominance on days 0 and 3 (99.56 ± 0.28% and 95.25 ± 2.61%, respectively). However, absolute abundance data revealed a marked expansion in *Bacillus* copy numbers, increasing from an average of 5.32×10^{10} copies/g on day 0 to 3.55×10^{12} copies/g on day 3. *Pantoea* and *Kosakonia* exhibited transient increases in biomass during the intermediate phases of the first and second fermentation stages (days 10–15 and day 38). *Pseudomonas* also showed a temporal increase on day 43 of the second fermentation stage, reaching an average of 8.58×10^{11} copies/g. In contrast, *Lelliottia*, *Enterobacter*, *Carnobacterium*, *Enterococcus*, and *Citrobacter* showed no clear stage-specific dynamics.

Among fungi, *Mucor* peaked on day 33 of the first fermentation stage with an average of 1.32×10^{12} copies/g. Other genera, including *Wickerhamomyces*, *Thelebolus*, and *Penicillium*, also showed noticeable increases during this period, whereas *Rhizopus* consistently remained predominant throughout both the first and second fermentation stages. Although *Aspergillus*, *Candida*, and *Gibberella* were included among the top 10 genera, they did not exhibit distinct temporal patterns during fermentation.

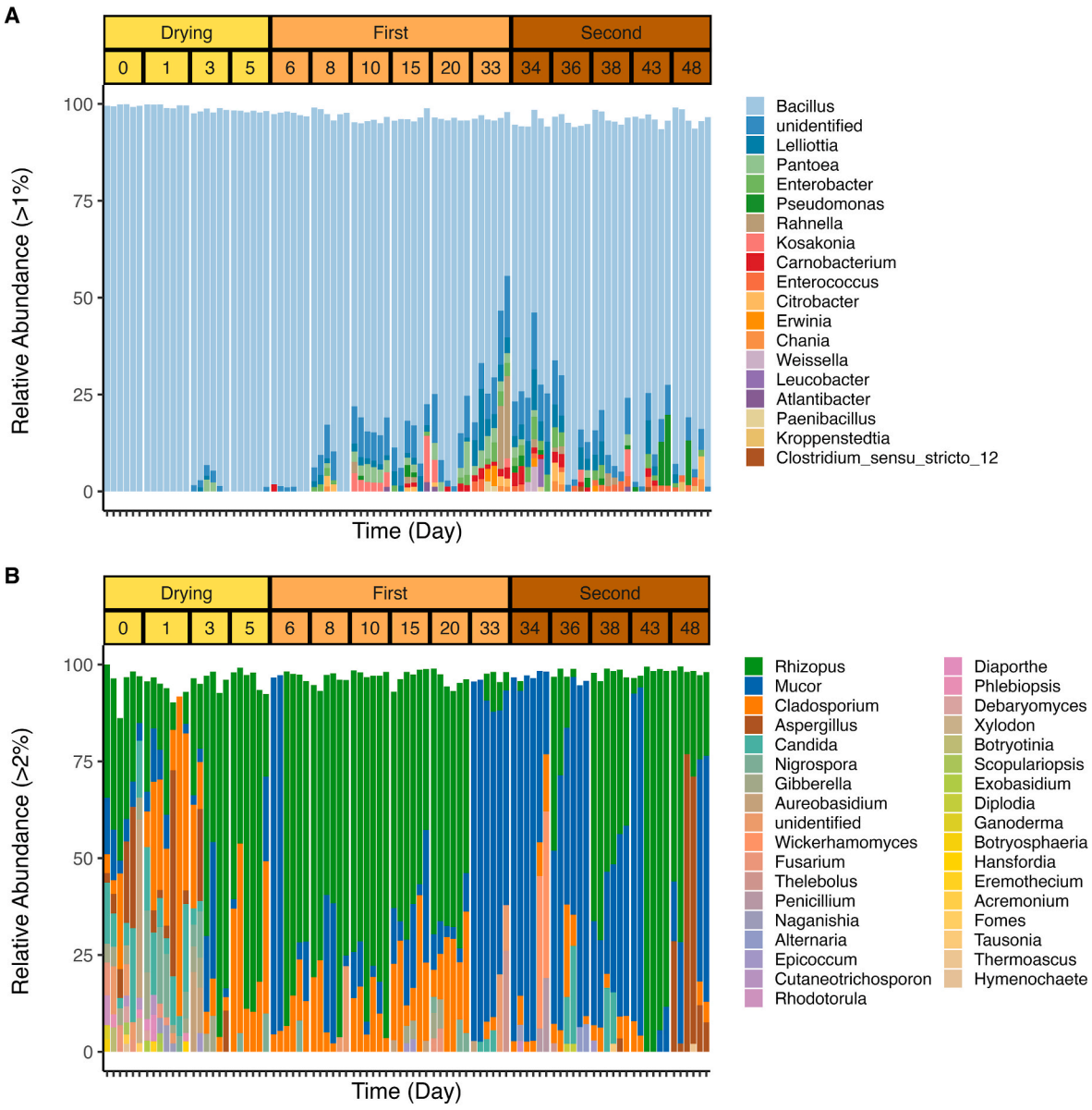

Fig. 4. Relative abundance of bacterial and fungal communities during *Meju* fermentation. Relative abundance of bacterial (A) and fungal (B) communities at the genus level. Amplicon sequence variants (ASVs) with <1% (bacteria) or < 2% (fungi) relative abundance were filtered. Fermentation stages and sampling days are indicated above each panel.

3.5. Bacterial-fungal correlations suggest mutualistic and competitive interactions in Meju fermentation

To elucidate the co-occurrence patterns and potential interactions between bacterial and fungal taxa during *Meju* fermentation, Spearman's correlation analyses were performed using both relative and absolute abundance data. The analysis focused on the top nine bacterial and nine fungal genera, excluding 'unidentified' taxa from the top 10 genera identified in both datasets. To identify significant correlations among these genera, a cutoff value of $|\rho| > 0.8$ with $p < 0.05$ was applied. Correlations among the selected genera were visualized as a network (Fig. 6).

When genera were represented as nodes and significant correlations as edges, a total of 47 significant correlations (26 positive and 21 negative) were identified based on relative abundance data (Fig. 6A). Notably, *Bacillus*, the most dominant bacterial genus, did not exhibit any significant correlations with other taxa in this analysis. In contrast, correlation analysis using absolute abundance data revealed 38 significant associations with 36 positive and 2 negative correlations (Fig. 6B). Specifically, *Bacillus* was positively correlated with *Rhizopus* ($\rho = 0.570$, $p = 0.03$) and negatively correlated with *Thelebolus* ($\rho = -1$, $p = 0.0$) and *Wickerhamomyces* ($\rho = -0.738$, $p = 0.04$). *Rhizopus* is known to secrete a wide range of carbohydrate-active enzymes, which may confer a growth advantage to *Bacillus* (Vellozo-Echevarría et al., 2024). In contrast, *Thelebolus,* which showed a significant negative correlation with *Bacillus*, has been reported to exhibit antibacterial activity against *Bacillus subtilis* (Nikitin et al., 2022). The significant correlation between *Bacillus* and various fungal taxa are consistent with its known metabolic diversity and secondary metabolite production capability. Although correlations alone cannot infer causality, they offer testable hypotheses that advance our ecological interpretation of microbial interactions.

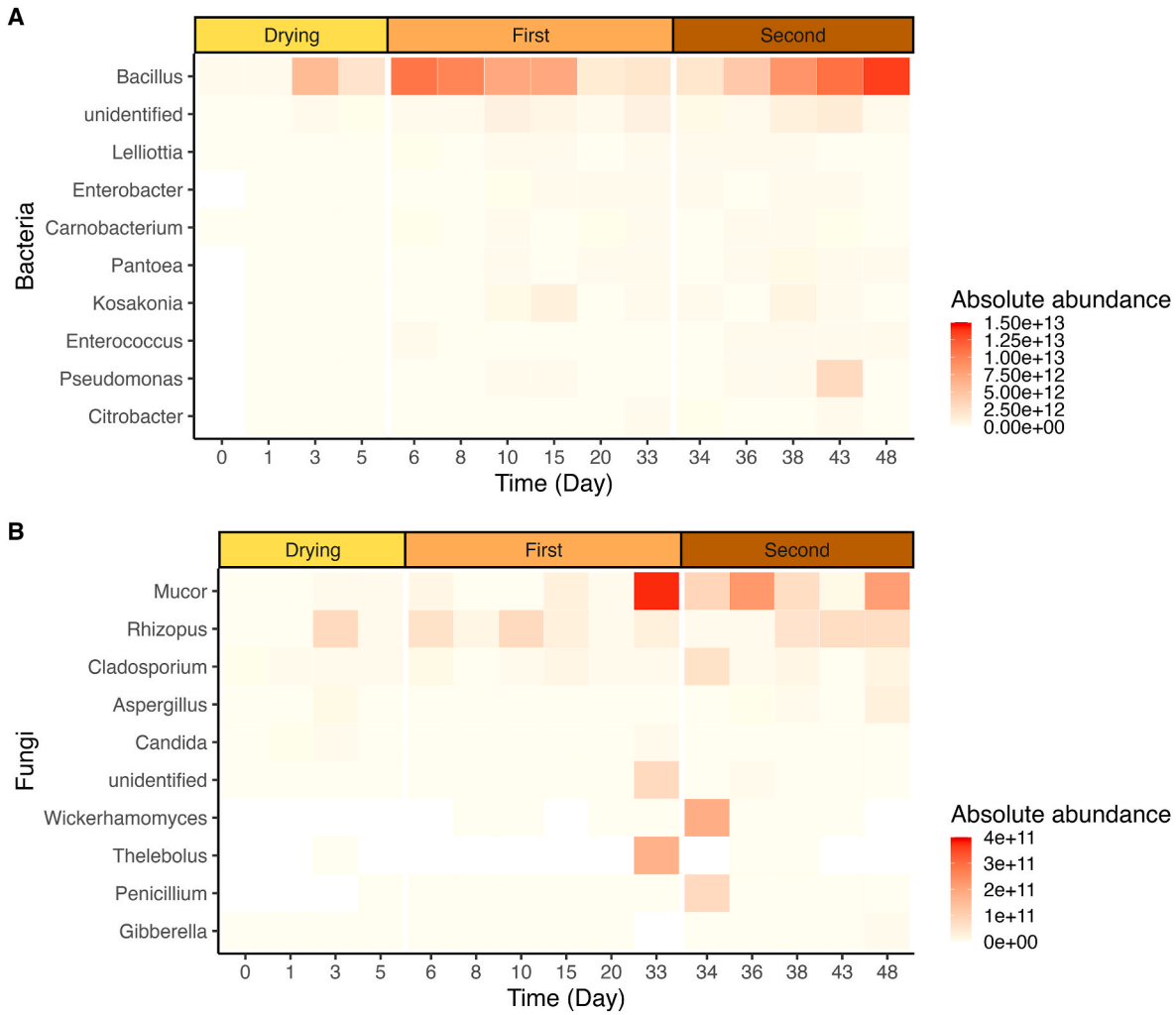

Fig. 5. Absolute abundance of bacterial and fungal taxa during *Meju* fermentation. Heatmaps of absolute abundance for 9 bacterial genera (A) and 9 fungal genera (B), including unidentified taxa. Each cell represents the abundance of a given taxon at a specific time point, visualized using a color gradient from ivory (low) to red (high).

4. Discussion

In this study, the progression of fermentation across the three stages of *Meju* production was evaluated by examining physicochemical parameters, such as pH, water content, and amino-type nitrogen contents, in conjunction with microbial biomass measurements. Bacterial and fungal dominants were identified across the three fermentation stages, and by integrating relative abundance profiles with quantitative data, absolute abundance estimates were obtained. This approach not only reflected changes in community composition but also captured increases in total microbial biomass, thereby providing a more accurate representation of microbial dynamics than relative data alone. This study revealed a potential biological interaction between *Bacillus* and *Rhizopus* during traditional *Meju* fermentation. While the findings are derived from samples obtained from a single manufacturer and therefore should not be generalized to all *Meju* products, this study nevertheless represents a rigorous integration of absolute microbial quantification and community-level analyses. By linking microbial biomass dynamics with ecological network analysis, this work provides meaningful insights into the interactions among dominant microorganisms in naturally fermented foods.

Physicochemical properties and microbial population dynamics were analyzed to elucidate the characteristics of each stage of *Meju* fermentation. Visual inspection of the *Meju* surface indicated active fungal growth accompanied by gradual color changes. During fermentation, the surface color transitioned to dark brown, which is likely attributable to the Maillard reaction, a nonenzymatic reaction between amino acids and reducing sugars derived from protein and polysaccharide degradation (Liu et al., 2022; Mottram et al., 2002). Additionally, enzymatic browning is known to be catalyzed by oxidoreductase released from microorganisms during soybean fermentation (Lertsiri et al., 2003; Park & Kyung, 1986). Temporal changes in *Meju* samples were characterized by a progressive decrease in water content accompanied by an increase in amino-type nitrogen, reflecting ongoing physiochemical transformations during fermentation. Quantification of bacterial and fungal target genes showed that microbial biomass increased by several orders of magnitude, reaching $\sim 10^{11}$ copies/g for bacteria and $\sim 10^{10}$ copies/g for fungi in the late stage of fermentation. These levels are comparable to those reported for Doenjang (Chun et al., 2020) and Chinese Doubanjiang (Yang et al., 2021), suggesting that the biomass expansion observed here is a common feature of soybean-based fermentations.

As a result of microbial diversity analysis, bacterial diversity increased, and the community composition shifted markedly during fermentation, likely due to the influx and establishment of diverse taxa. By contrast, the fungal community, after an initial increase in richness, was progressively dominated by a limited number of species that established ecological niches and constrained further diversification.

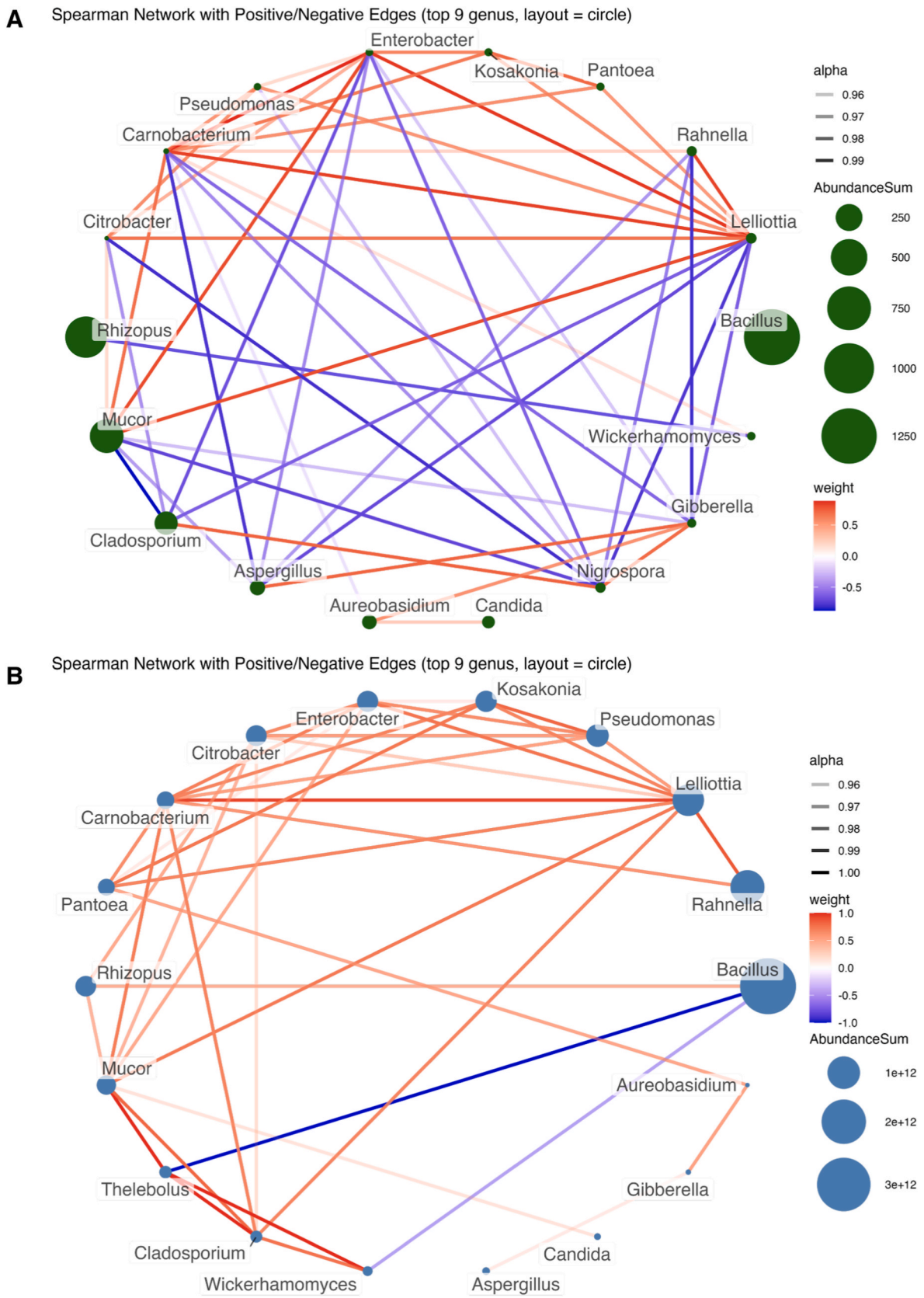

Fig. 6. Spearman's correlations between dominant bacterial and fungal taxa based on relative and absolute abundance data. Heatmaps of Spearman's correlations among the top nine bacterial and nine fungal genera, with red and blue indicating positive and negative correlations, respectively ($|\rho| > 0.5, p < 0.05$). Co-occurrence patterns inferred from relative (A) and absolute (B) abundance data are shown.

These contrasting trajectories underscore distinct ecological strategies of bacteria and fungi in *Meju* fermentation, where bacteria diversify and adapt dynamically, while fungi stabilize through competitive dominance.

Taxonomic profiling confirmed *Bacillus* as the predominant bacterial genus across three fermentation stages. Strains of *Bacillus* have been reported with major roles in proteolysis and amino nitrogen accumulation (Gil et al., 2022; Han et al., 2023). As another finding, the appearance of *Lelliottia, Pantoea, Enterobacter,* and *Rahnella* is interpreted as a result of open fermentation conditions influenced by the influx of microorganisms from the surrounding environment (Davin-Regli et al., 2019). Among fungi, *Rhizopus* and *Mucor* alternated in dominance, influenced by environmental conditions such as humidity, whereas *Aspergillus* was detected at lower levels compared with other studies (Oh et al., 2024; Ryu et al., 2021). Members of Zygomycota, including *Rhizopus* and *Mucor* at the genus level, have been identified in fermented soybean products through both culture-dependent and culture-independent approaches (Hong et al., 2012; Jung et al., 2014; Kim et al., 2011; Wikandari et al., 2012). Nevertheless, studies specifically addressing *Rhizopus* and *Mucor* remain limited, partly due to concerns about the potential pathogenicity of certain strains. According to a report, a comparative study of soybeans inoculated with *Mucor*, *Rhizopus*, and *Aspergillus*, either individually or in combination, demonstrated that *Mucor* significantly influenced volatile compound profiles, whereas *Rhizopus* affected the color characteristics of fermented soybeans (Heo et al., 2023). Collectively, these results emphasize that a comprehensive understanding of *Meju* fermentation requires elucidation of the interactions and functional characteristics among coexisting bacterial and fungal communities in this multi-microbial environment.

Capturing these interactions remains challenging when analyses rely exclusively on relative abundance data. Co-occurrence studies in fermented foods often rely solely on relative data, which represent microbial distributions as proportions totaling 100%, potentially leading to biased or misleading ecological inferences. To overcome this constraint, this study employed taxon-specific quantitative PCR targeting the 16S rRNA gene and ITS regions to obtain absolute abundance data, providing a more empirical framework for interpreting microbial population shifts during fermentation. While qPCR targeting the 16S rRNA gene or ITS region entails inherent methodological limitations, including primer bias, variation in rRNA gene copy number among taxa, and the inability to differentiate intracellular from extracellular DNA, it remains a powerful tool for capturing changes in total microbial biomass (Galazzo et al., 2020). Incorporating this quantitative information enables a more realistic interpretation of microbial distribution shifts during fermentation than reliance on relative abundance data alone.

A strong positive correlation emerged between the dominant *Bacillus* and *Rhizopus*, highlighting their potential ecological linkage during fermentation. This interkingdom association contrasts with previous *Meju* studies, which reported no significant correlations among dominants when using relative data (Kim et al., 2022). However, the presence of a significant positive correlation in this study implies that *Bacillus* and *Rhizopus* may engage in mutualistic interactions—potentially through protease activity and substrate modification—that support each other's growth, or share niches shaped by environmental filtering (Frey-Klett et al., 2011; Williams et al., 2014; Zhao et al., 2023). Experimental evidence indicates that co-cultivation with *Rhizopus* enhances the antibacterial capacity of *Bacillus* (Fukuda et al., 2008), which may create a more favorable niche for *Rhizopus* by inhibiting competing microbes. The findings of this study contribute to a deeper understanding of their potential symbiotic and functional roles in fermentation ecology.

Despite these insights, the observed associations remain inferential. Because correlation does not imply causation, correlation-based analyses should be interpreted as hypothesis-generating tools rather than definitive evidence of microbial interactions. Nevertheless, these analyses provide predictive insights into potential interactions among microbial taxa that are difficult to assess using traditional cultivation methods. Importantly, integrating absolute abundance measurements obtained by qPCR can mitigate biases associated with relative abundance data and strengthen ecological interpretations. In this context, our results suggest that an absolute abundance–informed framework represents a promising strategy for advancing a more rigorous, mechanistic understanding of microbial dynamics in traditional *Meju* fermentation. Furthermore, predicted interactions can be experimentally validated using coculture experiments with cultivable microbial species, thereby enabling a more mechanistic understanding of interactions between microorganisms.

Taken together, these results in this study emphasize that combining relative and absolute abundance data provides deeper insights into fermentation microbiomes than relative data alone. By capturing both microbial dynamics and biomass increases, this approach allowed us to detect hidden associations, particularly the *Bacillus–Rhizopus* link, that may play a central role in the ecology of *Meju* fermentation. This study provides a methodological framework for uncovering potential ecological relationships among dominant microorganisms in fermented foods and advances our understanding of inter-kingdom interactions underlying fermentation ecosystems.

CRediT authorship contribution statement

Eunhye Jo: Writing – original draft, Visualization, Software, Methodology, Investigation, Funding acquisition, Formal analysis, Data curation, Conceptualization. **Sungmin Hwang:** Writing – review & editing, Software. **Hyeyoung Lee:** Writing – review & editing, Supervision. **Jaeho Cha:** Writing – review & editing, Validation, Supervision, Project administration, Funding acquisition.

Funding sources

This research was supported by the National Research Foundation of Korea (NRF) grant funded by the Korean government (MSIT) (RS-2023-00247945), and by the Basic Science Research Program through the National Research Foundation of Korea (NRF), funded by the Ministry of Education (RS-2025-25438539).

Declaration of competing interest

The authors declare that they have no known competing financial interests or personal relationships that could have appeared to influence the work reported in this paper.

Acknowledgements

We thank Minjeong Kim and Taerim Kim for assisting experiments.

Appendix A. Supplementary data

Supplementary data to this article can be found online at https://doi.org/10.1016/j.fbio.2026.108444.

Data availability

Data will be made available on request.

References

Andrews, S. (2017). FastQC: A quality control tool for high-throughput sequence data. Retrieved from http://www.bioinformatics.babraham.ac.uk/projects/fastqc/. (Accessed 2 March 2023).

Beckers, B., Op De Beeck, M., Thijs, S., Truyens, S., Weyens, N., Boerjan, W., & Vangronsveld, J. (2016). Performance of 16s rDNA primer pairs in the study of rhizosphere and endosphere bacterial microbiomes in metabarcoding studies. *Frontiers in Microbiology, 7*(650), 1–15. https://doi.org/10.3389/fmicb.2016.00650

Bruijning, M., Ayroles, J. F., Henry, L. P., Koskella, B., Meyer, K. M., & Metcalf, C. J. E. (2023). Relative abundance data can misrepresent the heritability of the microbiome. *Microbiome, 11*(1), 222. https://doi.org/10.1186/s40168-023-01669-w

Bubeck, A. M., Preiss, L., Jung, A., Dörner, E., Podlesny, D., Kulis, M., Maddox, C., Arze, C., Zörb, C., Merkt, N., & Fricke, W. F. (2020). Bacterial microbiota diversity and composition in red and white wines correlate with plant-derived DNA contributions and botrytis infection. *Scientific Reports, 10*(1), Article 13828. https://doi.org/10.1038/s41598-020-70535-8

Callahan, B. J., McMurdie, P. J., Rosen, M. J., Han, A. W., Johnson, A. J., & Holmes, S. P. (2016). DADA2: High-resolution sample inference from illumina amplicon data. *Nature Methods, 13*(7), 581–583. https://doi.org/10.1038/nmeth.3869

Chun, B. H., Kim, K. H., Jeong, S. E., & Jeon, C. O. (2020). The effect of salt concentrations on the fermentation of doenjang, a traditional Korean fermented soybean paste. *Food Microbiology, 86*, Article 103329. https://doi.org/10.1016/j.fm.2019.103329

Davin-Regli, A., Lavigne, J. P., & Pagès, J. M. (2019). Enterobacter spp.: Update on taxonomy, clinical aspects, and emerging antimicrobial resistance. *Clinical Microbiology Reviews, 32*(4). https://doi.org/10.1128/cmr.00002-19. e00002-00019.

Elhalis, H., Chin, X. H., & Chow, Y. (2024). Soybean fermentation: Microbial ecology and starter culture technology. *Critical Reviews in Food Science and Nutrition, 64*(21), 7648–7670. https://doi.org/10.1080/10408398.2023.2188951

Frey-Klett, P., Burlinson, P., Deveau, A., Barret, M., Tarkka, M., & Sarniguet, A. (2011). Bacterial-fungal interactions: Hyphens between agricultural, clinical, environmental, and food microbiologists. *Microbiology and Molecular Biology Reviews, 75*(4), 583–609. https://doi.org/10.1128/mmbr.00020-11

Fukuda, T., Yamamoto, S., & Morita, H. (2008). Changes in the antibiotic production by co-culture of *Rhizopus peka* P8 and *Bacillus subtilis* IFO3335. *World Journal of Microbiology and Biotechnology, 24*(9), 1893–1899. https://doi.org/10.1007/s11274-008-9690-x

Galazzo, G., van Best, N., Benedikter, B. J., Janssen, K., Bervoets, L., Driessen, C., Oomen, M., Lucchesi, M., van Eijck, P. H., Becker, H. E. F., Hornef, M. W., Savelkoul, P. H., Stassen, F. R. M., Wolffs, P. F., & Penders, J. (2020). How to count our microbes? The effect of different quantitative microbiome profiling approaches. *Frontiers in Cellular and Infection Microbiology, 10*, 403. https://doi.org/10.3389/fcimb.2020.00403

Gil, N. Y., Jang, Y. J., Gwon, H. M., Jeong, W. S., Yeo, S. H., & Kim, S. Y. (2022). Comparative evaluation of quality and metabolite profiles in meju using starter cultures of *Bacillus velezensis* and *Aspergillus oryzae*. *Foods, 11*(68), 1–13. https://doi.org/10.3390/foods11010068

Han, D. M., Baek, J. H., Choi, D. G., & Jeon, C. O. (2024). Fermentative metabolic features of doenjang-meju as revealed by genome-centered metatranscriptomics. *Food Chemistry X, 23*, Article 101658. https://doi.org/10.1016/j.fochx.2024.101658

Han, D. M., Baek, J. H., Chun, B. H., & Jeon, C. O. (2023). Fermentative features of *Bacillus velezensis* and *Leuconostoc mesenteroides* in doenjang-meju, a Korean traditional fermented soybean brick. *Food Microbiology, 110*, Article 104186. https://doi.org/10.1016/j.fm.2022.104186

Harrell, F. E., Jr., & Dupont, C. (2019). Package 'hmisc'. Available from: https://CRAN.R-project.org/package=Hmisc.

Harrison, J. G., John Calder, W., Shuman, B., & Alex Buerkle, C. (2021). The quest for absolute abundance: The use of internal standards for DNA-based community ecology. *Molecular Ecology Resources, 21*(1), 30–43. https://doi.org/10.1111/1755-0998.13247

Heo, S., Park, J., Lee, K. G., Lee, J. H., & Jeong, D. W. (2023). Quality characteristics of soybean fermented by *Mucor, Rhizopus*, and *Aspergillus* from meju. *Heliyon, 9*(3), Article e14092. https://doi.org/10.1016/j.heliyon.2023.e14092

Hong, S. B., Kim, D. H., Lee, M., Baek, S. Y., Kwon, S. W., Houbraken, J., & Samson, R. A. (2012). Zygomycota associated with traditional meju, a fermented soybean starting material for soy sauce and soybean paste. *Journal of Microbiology, 50*(3), 386–393. https://doi.org/10.1007/s12275-012-1437-6

Jo, E., Lee, H., Song, Y., & Cha, J. (2024). Taxonomic variations of bacterial and fungal communities depending on fermentation temperature in traditional Korean fermented soybean food, doenjang. *Journal of Microbiology and Biotechnology, 34*(4), 863–870. https://doi.org/10.4014/jmb.2312.12024

Jung, J. Y., Lee, S. H., & Jeon, C. O. (2014). Microbial community dynamics during fermentation of doenjang-meju, traditional Korean fermented soybean. *International Journal of Food Microbiology, 185*, 112–120. https://doi.org/10.1016/j.ijfoodmicro.2014.06.003

Kallastu, A., Malv, E., Aro, V., Meikas, A., Vendelin, M., Kattel, A., Nahku, R., & Kazantseva, J. (2023). Absolute quantification of viable bacteria abundances in food by next-generation sequencing: Quantitative NGS of viable microbes. *Current Research in Food Science, 6*, Article 100443. https://doi.org/10.1016/j.crfs.2023.100443

Kim, D. H., Chun, B. H., Lee, J. J., Kim, O. C., Hyun, J., Han, D. M., Jeon, C. O., Lee, S. H., Lee, S. H., Choi, Y. H., & Hong, S. B. (2024). Enzymatic activity and amino acids production of predominant fungi from traditional meju during soybean fermentation. *Journal of Microbiology and Biotechnology, 34*(3), 654–662. https://doi.org/10.4014/jmb.2309.09008

Kim, H. M., Han, D., Baek, J. H., Chun, B. H., & Jeon, C. O. (2022). Dynamics and correlation of microbial communities and metabolic compounds in doenjang-meju, a Korean traditional soybean brick. *Food Research International, 155*, Article 111085. https://doi.org/10.1016/j.foodres.2022.111085

Kim, D. H., Kim, S. H., Kwon, S. W., & Lee, J. K. (2013). Fungal diversity of rice straw for meju fermentation. *Journal of Microbiology and Biotechnology, 23*(12), 1654–1663. https://doi.org/10.4014/jmb.1307.07071

Kim, K. M., Lim, J., Lee, J. J., Hurh, B. S., & Lee, I. (2017). Characterization of *Aspergillus sojae* isolated from meju, Korean traditional fermented soybean brick. *Journal of Microbiology and Biotechnology, 27*(2), 251–261. https://doi.org/10.4014/jmb.1610.10013

Kim, J. Y., Yeo, S. H., & Baek, S. Y. (2011). Molecular and morphological identification of fungal species isolated from bealmijang meju. *Journal of Microbiology and Biotechnology, 21*(12), 1270–1279. https://doi.org/10.4014/jmb.1105.05013

Lee, H., Jo, E., Song, J., Min, J., Song, Y., Lee, H., Choe, Y., Cha, J., & Lee, H. (2024). Correlation between monosaccharide, oligosaccharide, and microbial community profile changes in traditional soybean brick (Meju) fermentation. *Food Research International, 184*, Article 114233. https://doi.org/10.1016/j.foodres.2024.114233

Lertsiri, S., Phontree, K., Thepsingha, W., & Bhumiratana, A. (2003). Evidence of enzymatic browning due to laccase-like enzyme during mash fermentation in Thai soybean paste. *Food Chemistry, 80*(2), 171–176. https://doi.org/10.1016/S0308-8146(02)00251-0

Liu, S. Y., Sun, H. J., Ma, G., Zhang, T., Wang, L., Pei, H., Li, X., & Gao, L. Y. (2022). Insights into flavor and key influencing factors of Maillard reaction products: A recent update. *Frontiers in Nutrition, 9*, Article 973677. https://doi.org/10.3389/fnut.2022.973677

McMurdie, P. J., & Holmes, S. (2013). Phyloseq: An R package for reproducible interactive analysis and graphics of microbiome census data. *PLoS One, 8*(4), Article e61217. https://doi.org/10.1371/journal.pone.0061217

Mennah-Govela, Y. A., Cai, H. C., Chu, J., Kim, K., Maborang, M. K., Sun, W. Y., & Bornhorst, G. M. (2020). Buffering capacity of commercially available foods is influenced by composition and initial properties in the context of gastric digestion. *Food & Function, 11*(3), 2255–2267. https://doi.org/10.1039/c9fo03033f

Mottram, D. S., Wedzicha, B. L., & Dodson, A. T. (2002). Acrylamide is formed in the Maillard reaction. *Nature, 419*(6906), 448–449. https://doi.org/10.1038/419448a

Na, H. E., Heo, S., Kim, Y. S., Kim, T., Lee, G., Lee, J. H., & Jeong, D. W. (2022). The safety and technological properties of *Bacillus velezensis* DMB06 used as a starter candidate were evaluated by genome analysis. *LWT - Food Science and Technology, 161*, Article 113398. https://doi.org/10.1016/j.lwt.2022.113398

Nikitin, D. A., Sadykova, V. S., Kuvarina, A. E., Dakh, A. G., & Biryukov, M. V. (2022). Enzymatic and antimicrobial activities in polar strains of microscopic soil fungi. *Doklady Biological Sciences, 507*(1), 380–393. https://doi.org/10.1134/S0012496622060151

Nilsson, R. H., Larsson, K.-H., Taylor, A. F. S., Bengtsson-Palme, J., Jeppesen, T. S., Schigel, D., Kennedy, P., Picard, K., Glöckner, F. O., Tedersoo, L., Saar, I., Kõljalg, U., & Abarenkov, K. (2019). The UNITE database for molecular identification of fungi: Handling dark taxa and parallel taxonomic classifications. *Nucleic Acids Research, 47*(D1), D259–D264. https://doi.org/10.1093/nar/gky1022

Oh, S. J., Kang, G. S., Lee, H. R., Yu, S. J., Jeong, S. U., So, Y. S., Park, C. S., Shin, D., & Seo, D. H. (2024). Microbial communities in the fermentation of Meju, a Korean traditional soybean brick. *Food Science and Biotechnology, 33*, 2815–2823. https://doi.org/10.1007/s10068-024-01531-1

Op De Beeck, M., Lievens, B., Busschaert, P., Declerck, S., Vangronsveld, J., & Colpaert, J. V. (2014). Comparison and validation of some ITS primer pairs useful for fungal metabarcoding studies. *PLoS One, 9*(6). https://doi.org/10.1371/journal.pone.0097629. e97629-e97629.

Park, S. K., & Kyung, K. H. (1986). Pigment-forming bacteria in the presence of L-tyrosine and their possible role in the browning of fermented soybean products. *Korean Journal of Food Science and Technology, 18*(5), 376–381.

Props, R., Kerckhof, F. M., Rubbens, P., De Vrieze, J., Hernandez Sanabria, E., Waegeman, W., Monsieurs, P., Hammes, F., & Boon, N. (2017). Absolute quantification of microbial taxon abundances. *The ISME Journal: Multidisciplinary Journal of Microbial Ecology, 11*(2), 584–587. https://doi.org/10.1038/ismej.2016.117

Quast, C., Pruesse, E., Yilmaz, P., Gerken, J., Schweer, T., Yarza, P., Peplies, J., & Glöckner, F. O. (2012). The SILVA ribosomal RNA gene database project: Improved data processing and web-based tools. *Nucleic Acids Research, 41*(D1), D590–D596. https://doi.org/10.1093/nar/gks1219

Ryu, J. A., Kim, E., Yang, S. M., Lee, S., Yoon, S. R., Jang, K. S., & Kim, H. Y. (2021). High-throughput sequencing of the microbial community associated with the physicochemical properties of meju (dried fermented soybean) and doenjang (traditional Korean fermented soybean paste). *LWT - Food Science and Technology, 146*, 111473–111481. https://doi.org/10.1016/j.lwt.2021.111473

Shanahan, F., & Hill, C. (2019). Language, numeracy, and logic in microbiome science. *Nature Reviews Gastroenterology & Hepatology, 16*(7), 387–388. https://doi.org/10.1038/s41575-019-0163-5

Shin, D., & Jeong, D. (2015). Korean traditional fermented soybean products: Jang. *Journal of Ethnic Foods, 2*(1), 2–7. https://doi.org/10.1016/j.jef.2015.02.002

Singh, D., Lee, S. H., & Lee, C. H. (2022). Non-obligate pairwise metabolite cross-feeding suggests ammensalic interactions between *Bacillus amyloliquefaciens* and *Aspergillus oryzae*. *Communications Biology, 5*(1), 232. https://doi.org/10.1038/s42003-022-03181-7

Song, D. H., Chun, B. H., Lee, S., Reddy, C. K., Jeon, C. O., & Lee, C. H. (2020). Metabolite profiling and microbial community of traditional meju show primary and secondary metabolite differences correlated with antioxidant activities. *Journal of Microbiology and Biotechnology, 30*(11), 1697–1705. https://doi.org/10.4014/jmb.2007.07026

Song, D. H., Chun, B. H., Lee, S., Son, S. Y., Reddy, C. K., Mun, H. I., Jeon, C. O., & Lee, C. H. (2021). Comprehensive metabolite profiling and microbial communities of doenjang (fermented soy paste) and ganjang (fermented soy sauce): A comparative study. *Foods, 10*(3), 641–655. https://doi.org/10.3390/foods10030641

Sun, X., Lyu, G., Luan, Y., Yang, H., & Zhao, Z. (2019). Metabolomic study of the soybean pastes fermented by the single species *Penicillium glabrum* GQ1-3 and *Aspergillus oryzae* HGPA20. *Food Chemistry, 295*, 622–629. https://doi.org/10.1016/j.foodchem.2019.05.162

Taylor, W. (1957). Formol titration: An evaluation of its various modifications. *Analyst, 82*(976), 488–498. https://doi.org/10.1039/AN9578200488

Vandeputte, D., Kathagen, G., D'hoe, K., Vieira-Silva, S., Valles-Colomer, M., Sabino, J., Wang, J., Tito, R. Y., De Commer, L., Darzi, Y., Vermeire, S., Falony, G., & Raes, J. (2017). Quantitative microbiome profiling links gut community variation to microbial load. *Nature, 551*(7681), 507–511. https://doi.org/10.1038/nature24460

Vellozo-Echevarría, T., Barrett, K., Vuillemin, M., & Meyer, A. S. (2024). The distinct carbohydrate-active enzyme secretome of *Rhizopus* spp. represents fitness for mycelium remodeling and solid-state plant food fermentation. *ACS Omega, 9*(32), 34185–34195. https://doi.org/10.1021/acsomega.4c04378

Wikandari, R., Millati, R., Lennartsson, P. R., Harmayani, E., & Taherzadeh, M. J. (2012). Isolation and characterization of zygomycete fungi from tempe for ethanol production and biomass applications. *Applied Biochemistry and Biotechnology, 167*(6), 1501–1512. https://doi.org/10.1007/s12010-012-9587-x

Williams, R. J., Howe, A., & Hofmockel, K. S. (2014). Demonstrating microbial co-occurrence pattern analyses within and between ecosystems. *Frontiers in Microbiology, 5*(358), 1–10. https://doi.org/10.3389/fmicb.2014.00358

Yang, Y., Niu, C. T., Shan, W. X., Zheng, F. Y., Liu, C. F., Wang, J. J., & Li, Q. (2021). Physicochemical, flavor, and microbial dynamic changes during low-salt doubanjiang (broad bean paste) fermentation. *Food Chemistry, 351*, Article 128454. https://doi.org/10.1016/j.foodchem.2020.128454

Yang, K., Su, W., Mu, Y., Liu, X., Liu, Y., & Lu, Y. (2025). Microbial absolute quantification and metabolomics reveal the impact of partial KCl substitution for NaCl on the flavor quality of Zao Chili. *Food Bioscience, 68*, Article 106495. https://doi.org/10.1016/j.fbio.2025.106495

Yang, L., Xian, C., Li, P., Wang, X., Song, D., Zhao, L., & Zhang, C. (2023). The spatio-temporal diversity and succession of microbial community and its environment driving factors during the stacking fermentation of Maotai-flavor baijiu. *Food Research International, 169*, Article 112892. https://doi.org/10.1016/j.foodres.2023.112892

Zhao, Y., Liu, Z., Zhang, B., Cai, J., Yao, X., Zhang, M., Deng, Y., & Hu, B. (2023). Inter-bacterial mutualism is promoted by public goods in a system characterized by deterministic temperature variation. *Nature Communications, 14*(1), 5394. https://doi.org/10.1038/s41467-023-41224-7